Optical DC Transformers Incorporating Improved Sensing Cell Materials and Signal Processing

Jinfeng Luo*

School of Automotive and Mechanical and Electrical Engineering
Xinyang Vocational and Technical College, Xinyang 464000, China

ABSTRACT: Optical direct current (DC) transformer has become a hot spot of research with its high accuracy, wide bandwidth, and high voltage isolation characteristics, but has the technical difficulties of low signal-to-noise ratio of ODCT signal and poor temperature stability. For this reason, the study proposes a new type of optical DC transformer integrating material science and signal processing. The study introduces an improved terbium gallium garnet crystal sensing unit material and a signal processing algorithm with a plus-window dual correlation detection algorithm, and constructs an optical DC transformer model. Simulation results show that the temperature compensation method can effectively weaken the influence of temperature change on the measurement accuracy under both warming and cooling conditions, and higher accuracy can be obtained by using the whole period window for measurement. The system applying terbium gallium garnet crystals helps to enhance the measuring system's output signal-to-noise ratio and sensitivity. Terbium gallium garnet crystals as a sensing material can further decrease the measuring error compared with other magneto-optical glasses. Taken together, DC measurement system using terbium gallium garnet crystals and dual correlation detecting algorithm can control the error to about 0.3 s. Simulation experiments verify the validity and feasibility of the research methodology, which can guide the research and application of optical DC transformers in the future.

1. INTRODUCTION

With the continuous development of power systems and high-precision measurement technology, there are higher requirements for the performance of transformer. Traditional current transformers have limitations in DC measurement, such as low accuracy and slow response time [1]. In recent years, the development of new sensor materials has opened up the possibility of improving the performance of the transformers. These materials typically have better sensitivity, wider response frequency range, and higher stability. Advances in signal processing techniques have made it possible to extract more accurate information from complex signals, which is critical to the accuracy and reliability of current measurements [2]. Optical DC transformers are devices that use optical methods to measure DC. Unlike conventional current transformers, optical DC transformers offer many advantages, including high dielectric strength, wide-band response, and strong immunity to electromagnetic field interference [3]. The novelty of this research lies in the improved sensor materials and signal processing techniques that enable optical DC transformers to achieve higher measurement accuracy, especially in low frequency and DC applications. This research has four main parts. At first, there is a literature review, which summarises the current research results on DC measurement of transformers and other aspects. The second part is the research methodology, including the material improvement of the sensing unit based on Terbium Gallium Garnet (TGG) crystals, the signal processing based on the

plus-window bicorrelation detection algorithm, and the model construction of the optical DC transformer. The third part is the result analysis, which focuses on the simulation analysis of the research method. The fourth part is the conclusion, which summarises the research results and shortcomings.

2. RELATED WORKS

Due to the development of power systems and measurement techniques, higher performance transformers are required to meet the challenges of DC measurement. In order to eliminate the capacitive voltage deviation in DC sub-transformers, a sub-module capacitance equalisation method based on dual active bridges is proposed to reduce the capacitive voltage stress. The results show that the method is able to provide effective elimination of capacitive voltage deviation and meets the different needs of medium-voltage and high-voltage application scenarios [4]. Zhuo et al. proposed a power electronic transformer-based control method to improve the structure of the dual active bridge module of the contributing DC transformer in order to deal with the difficulty of current limitation in the DC power grid. The results show that the method is capable of actively controlling the current output from the transformer to meet the requirements of renewable energy power generation equipment [5]. Wang et al. proposed a multi-short flexible DC distribution protection system based on transient current curvature in response to the problem of the DC distribution system's short time for identifying the fault transient cycle. The experimental results show that the method can improve the identi-

---

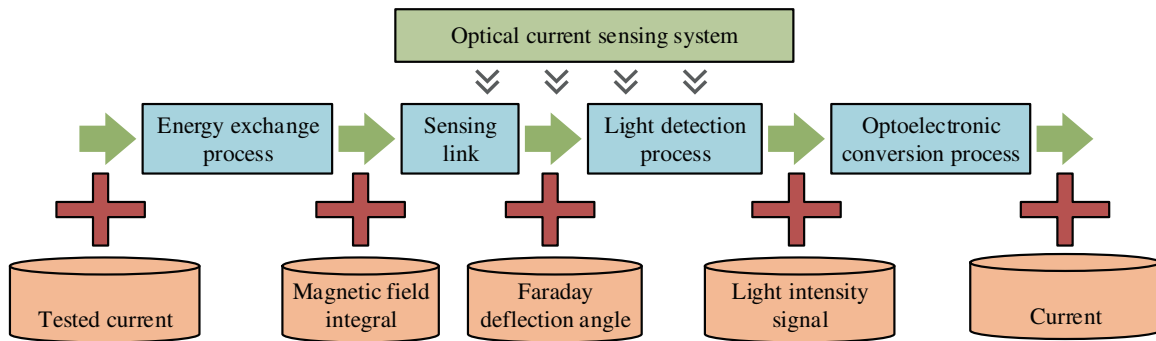* Corresponding author: Jinfeng Luo (luojinfeng_2001@163.com).

FIGURE 1. Structure of optical current sensing system.

fication accuracy of internal high resistance faults and meet the speed and reliability requirements of DC distribution systems [6]. In order to solve the problem of DC flowing into the grid without current isolation, researchers designed a DC voltage detection method based on a two-stage DC voltage detection technique and a filtering algorithm. The research results show that the method is able to actively control the current and effectively extract and suppress the DC voltage [7].

For the problem of current under grid voltage such as transformers, many other scholars have carried out corresponding researches to improve the accuracy of the current measurement to meet more application scenarios. In order to analyse the three-phase five-bridge-arm transformer with DC bias under grid voltage, an analytical model based on the frequency-dependent reluctance model is proposed by researchers. Experimental results show that high permeability or low reluctance transformer core materials lead to higher excitation currents at saturation [8]. In order to reduce the voltage and current ripple inputs to a photovoltaic system, a boosted half-bridge DC-DC converter was designed by connecting an auxiliary capacitor in series to the primary coil of a 1 : 1 transformer. The results of the study show that the method is able to reduce the input voltage and current ripples and can be applied to different input voltages and currents [9]. Achlerkar and Panigrahi have proposed a least error squared based evaluation method to correct the DC signal model in order to evaluate the offset of the DC component in the fault current signal. The research results show that the method is able to locate the phase quantities more accurately and is significantly better than the current DC offset estimation method [10]. Geng et al. designed a new mechanism based on inductive excitation of high DC high temperature superconducting magnets in response to the fact that the coarse current leads of the high temperature superconducting magnets generate a large thermal load in a low-temperature environment. The experimental results show that the research method can satisfy the need to work in a closed low-temperature environment, eliminating the need for an electronic power supply and bulky current leads [11].

Optical DC transformers have extremely important application value in areas such as high voltage detection of power systems, and the research and application of optical DC transformers can promote the modernisation of power systems. Providing more accurate current data contributes to the stable operation of the power grid and timely troubleshooting. In view of this, this research will be conducted by using advanced sensor materials and signal processing techniques in order to improve the accuracy of current measurements, promote the modernisation of power systems, improve the intelligence and stability of power grids, and also potentially promote technological advances in related fields such as new energy and smart grids.

3. CONSTRUCTION OF IMPROVED OPTICAL DC TRANSFORMER MODEL

In order to enhance the correlation performance of the optical DC transformer, the study introduces improved sensing unit materials and signal processing algorithms, which improve crystal sensing unit materials and signal processing algorithms with the addition of a windowed dual correlation detection algorithm, respectively, and constructs a model of the optical DC transformer.

3.1. Material Improvement of Sensing Unit Based on TGG Crystal

Optical DC transformers, as a device for measuring DC by optical means, offer a variety of advantages not found in conventional current transformers, such as strong immunity to electromagnetic field interference. These transformers usually make use of the Faraday effect, in which a magnetic field in the path of light propagation causes polarised light passing through the medium to rotate at an angle proportional to the current passing through the medium. By measuring the angle of rotation of the polarised light, the value of the DC flowing through the conductor can be derived [12]. By building a mathematical model of each part of the optical current sensing system, the inputs and outputs of each link can be analysed at a system level. In an optical current sensing system, the process of performing a DC measurement is shown in Fig. 1 [13, 14].

As can be seen in Fig. 1, the optical current sensing system DC measurement involves four key steps. Firstly, the transducer link converts the measured DC into magnetic induction intensity, a process that depends on the position of the current [15]. Second, the sensing link receives the magnetic induction intensity and converts it into a Faraday deflection angle that modulates the line-polarised light. Next, in the light detec-

tion link, the Faraday deflection angle is converted into a light intensity signal. Finally, the photoconversion link converts the light intensity signal into a voltage signal for subsequent signal processing and analysis.

Magneto-optical materials, as functional materials, exhibit magneto-optical effects in the visible and infrared light bands and are widely used in optical devices such as optical isolation and optical modulation. Such materials play a key role in the performance of optical current transformers, especially through their Fielder constant and temperature characteristics. The larger the Fielder constant is, the higher the Faraday deflecting angle and the measuring sensitivity and Signal-to-noise Ratio (SNR) of the transformer are. The study proposes the use of a paramagnetic magneto-optical material, TGG crystals, which have a high Fielder's constant and can reduce the length of the required material while improving SNR and the measuring sensitivity, thus reducing the effect of linear birefringence [16, 17]. TGG is a paramagnetic material widely used in magneto-optical applications, especially as a magneto-optical crystal in high-performance far-infrared optical isolators. Although TGG itself does not exhibit spontaneous magnetization as a paramagnetic material, its magneto-optical interaction can be excited by an external magnetic field. In the absence of an external magnetic field, the magnetic moment of terbium (Tb) ions in TGG is randomly arranged and does not produce macroscopic magnetization phenomena. However, when a magnetic field is applied, the magnetic moment of paramagnetic terbium ions in TGG tends to align along the direction of the magnetic field, resulting in macroscopic magnetization of the material. At this point, the light passing through TGG will undergo a magneto-optical effect, known as Faraday rotation, and the polarization plane of the light will rotate around the direction of the magnetic field during the process of passing through the material [18]. The angle of Faraday rotation is directly proportional to the thickness of the material passing through, the magneto-optical constant of the material, and the applied magnetic field strength. Therefore, although TGG is a paramagnetic material and does not exhibit magnetic response in the absence of an external magnetic field, its magneto-optical interaction can be excited by applying a magnetic field. Since the Fielder constant of magneto-optical materials is a key indicator of their performance, the study will analyse the TGG crystal's Fielder constant in detail, and its expression is shown in Equation (1).

$$V = V_{dm} + V_{mix} + V_{pm} + V_{gm} \qquad (1)$$

In Equation (1), V denotes the Fielder's constant of TGG crystals, and V_{dm} and V_{mix} are components that have no relationship with temperature. When there are paramagnetic ions in TGG crystals, V_{dm} is negligible. V_{pm} represents the paramagnetic term, which plays an important role in Fielder constant; V_{gm} is derived from the magnetic dipole transition, which is related to the temperature. Combined with the expressions of V_{mix}, V_{pm}, and V_{gm}, the Fielder's constant of TGG crystal is shown in Equation (2) when the wavelength of incident light is certain.

$$V(T) = \frac{G}{T - T_w} + H \qquad (2)$$

In Equation (2), T denotes the resistance temperature, T_w the Curie temperature of the material, H the magnetic field strength in units of (A/m), and G the constant related to the material. The Fielder's constant of the TGG crystals decreases at increasing temperatures, and this change is significant, making the crystals susceptible to external temperature fluctuations. Considering that optical DC transformers are often deployed in harsh environments with large temperature variations, it is particularly important to develop an effective temperature compensation mechanism to reduce the negative impact of temperature variations on measurement accuracy [15]. When temperature fluctuations are considered, Equation (3) is utilised to represent the output signal of this measurement system.

$$u_0(T) = V(T) I = K_1(T) I \qquad (3)$$

In Equation (3), $K_1(T)$ denotes the responsivity of optical coherence tomography when temperature fluctuations are considered, which is more related to the Fielder constant of the sensing material. I denotes the average value of the current flowing through the conductor contact surface in A; u_0 is the noise voltage [19]. The specific difference of the DC transformer is shown in Equation (4).

$$\varepsilon = \frac{K(T) I - K(T_0) I_0}{K(T_0) I_0} \qquad (4)$$

In Equation (4), ε denotes the specific difference of the DC transformer. In this study, room temperature 293 K was used as the standard temperature, so at the standard temperature, the initial specific difference is shown in Equation (5).

$$\varepsilon_0 = \frac{K(T_0) I - K(T_0) I_0}{K(T_0) I_0} \qquad (5)$$

In Equation (5), ε_0 denotes the initial specific difference. In turn, the specific difference when the temperature changes can be obtained, and the expression is shown in Equation (6).

$$\varepsilon = \varepsilon_0 + \Delta\varepsilon \qquad (6)$$

In Equation (6), $\Delta\varepsilon$ indicates the specific difference caused by temperature fluctuation. It is considered that the specific difference is close to 0 at the standard temperature, and the specific difference generated with temperature change is shown in Equation (7).

$$\Delta\varepsilon = \left[\frac{K(T)}{K_0} - 1\right] \qquad (7)$$

Since temperature variations lead to measurement errors, it is equivalent to adding a temperature-dependent interference signal to the measured DC signal. Therefore, temperature compensation is performed by adding a temperature compensation link to the signal processing unit to superimpose a compensation signal with the same value as the interfering signal but with the opposite sign to counteract the interference, whose specific expression can be seen in Equation (8).

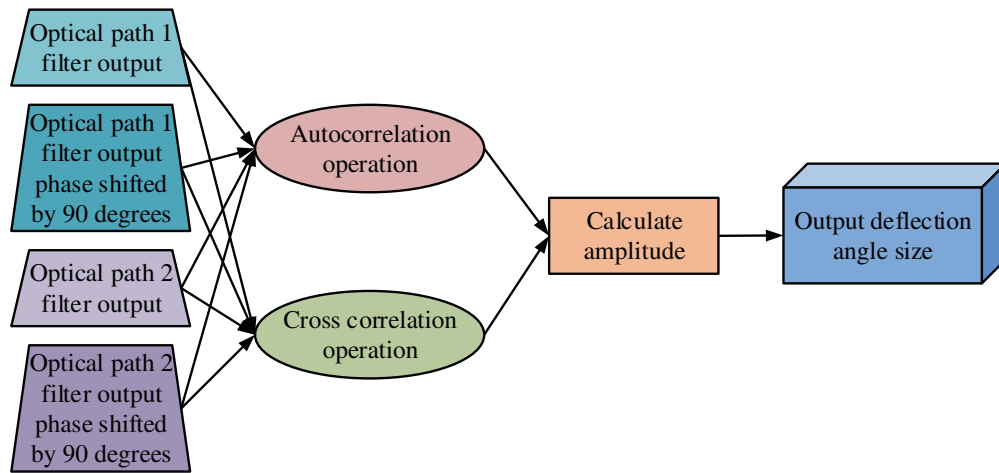$$u(T) = u_0 + \Delta u(T) + u_c \qquad (8)$$

FIGURE 2. Process of double correlation detecting algorithm.

In Equation (8), u_c is the temperature compensation signal. Then the amount of error in responsivity drift with temperature is shown in Equation (9).

$$\Delta K\left(T\right) = K_0 \Delta \varepsilon \qquad (9)$$

In turn, the temperature compensation signal can be obtained, and the expression is shown in Equation (10).

$$u_c = -\Delta u\left(T\right) = -K_0 I \Delta \varepsilon \qquad (10)$$

This completes the temperature compensation.

3.2. Signal Processing Based on Plus Window Bicorrelation Detection Algorithm

In order to cope with the challenge of low SNR of the output signal, the use of TGG crystals with higher Fielder's constant as the sensing material will achieve better results. However, only enhancing the Faraday deflecting angle cannot completely solve the problems of low SNR and overlapping signal-to-noise bands. Therefore, based on the weak signal detection technique, a dual correlation detection algorithm is proposed. The algorithm first separates the signal-to-noise band, then eliminates the low-frequency noise through the filter, and removes the white noise using the algorithm, thus enhancing SNR and improving the performance of the transformer. For the measurement of transient signals, a dual correlation detection method with a window is developed.

Optical DC sensors based on the Faraday magneto-optical effect encounter difficulties in signal detection, where the signal amplitude is weak, close to the noise amplitude and overlapping in frequency bands, resulting in a very low SNR [20]. Although TGG crystals with high Fielder's constant are used, SNR still exists. For this reason, a dual correlation detection method combining multiple autocorrelation and lock-in amplification techniques is used to effectively separate the weak signal from the noise and solve the challenges of low SNR and band overlap. The process of the dual correlation detection algorithm is shown in Fig. 2.

In Fig. 2, the correlation detection method utilises autocorrelation function and cross-correlation function, where the periodic signals $x\left(t\right)$ and $y\left(t\right)$ with the same frequency, their autocorrelating and cross-correlating functions are shown in Equation (11).

$$\begin{cases} R_{xx}\left(\tau\right) = E\left[x\left(t-\tau\right)x\left(t\right)\right] \\ \\ \qquad = \lim_{T \to \infty} \dfrac{1}{T} \displaystyle\int_0^T x\left(t-\tau\right)x\left(t\right)dt \\ \\ R_{xy}\left(\tau\right) = E\left[x\left(t-\tau\right)y\left(t\right)\right] \\ \\ \qquad = \lim_{T \to \infty} \dfrac{1}{T} \displaystyle\int_0^T x\left(t-\tau\right)y\left(t\right)dt \end{cases} \qquad (11)$$

In Equation (11), T denotes the period of the cyclic signals $x\left(t\right)$ and $y\left(t\right)$, and τ is the delay of the signal. In order to separate the signal from the low-frequency noise, DC signal is first converted to a high-frequency signal using a spectral migration technique, which is used as the input to the signal processing [21]. The autocorrelation function of the white noise is concentrated at $t = 0$, while it tends to zero when t tends to infinity and can therefore be ignored. By analysing the processed signal, the amplitude of the original DC signal can be accurately measured. Aiming at the inadequacy of the existing double correlation detection algorithm in analysing transient signals, the study proposes an improved algorithm. Considering the short-time nature of transient signals, a dual correlation detection method with added windows is developed by combining the principles of Gabor transform and short-time Fourier transform. This method divides the transient signal into multiple time segments by analysing the signal in different time windows, and the signal is regarded as stable in each segment, so as to carry out effective bicorrelation analysis in each time segment, which improves the accuracy and reliability of the transient signal detection. Assuming that $f\left(t\right)$ denotes the transient signal, and the window function is expressed using the rectangular window function, then the expression of the window

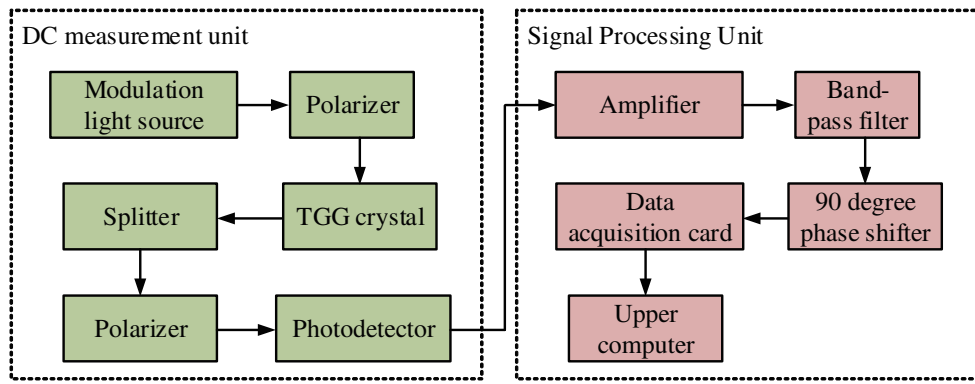**FIGURE 3**. The basic framework of optical DC measurement systems.

function is shown in Equation (12).

$$g_a\left(t-b\right) = \begin{cases} 1, & b - \dfrac{a}{2} \le t < b + \dfrac{a}{2} \\ 0, & t < b - \dfrac{a}{2} \ or \ t \ge \dfrac{a}{2} \end{cases} \qquad (12)$$

In Equation (12), b and a denote the translation factor and the width of the window function, respectively, and then the signal after adding the window is shown in Equation (13).

$$f_b\left(t\right) = f\left(t\right) * g_a\left(t-b\right) \qquad (13)$$

Transient signals can be effectively detected by applying the sliding window function, adding a window to the signal, and performing the double correlation analysis mentioned previously.

3.3. Optical DC Transformer Modelling Incorporating Improved Sensing Unit Materials and Signal Processing

In order to study the performance of the optical DC measurement system, the system model was established, and the corresponding hardware circuit, optical path, and software were designed. The experimental platform is divided into steady state and transient parts for testing different types of DC and comparing the effects of different materials and signal processing algorithms. Fig. 3 shows the basic framework of the optical DC measuring system.

As can be seen in Fig. 3, the DC measurement system is divided into two main parts, DC measurement and signal processing. The DC measurement part includes a modulated light source, a sensor unit, and a photodetector. The modulated lighting source is used to generate a spectrally migrated high-frequency optical signal. The sensor unit selects a TGG crystal as a sensing material and adopts a straight-through optical path structure, which reduces the influence of the fluctuation of the modulated light source on the measurement accuracy through the dual optical path design. The filtered signals are further processed using the dual correlation detection algorithm [22]. A 90°phase shifter is used to generate the shift signals required for the dual correlation detection, and the data acquisition card collects the signals to be processed in the Labview software of the host computer to finally obtain the accurate signals to be

measured. In this way, the two light intensity signals derived from the modulated lighting source and the sensing part are converted into voltage signals, and the centre frequency of the band-pass filter is set to the modulation frequency. After filtering, the signals that have been filtered out of the low-frequency noise, most of the white noise, the DC component can be obtained. The expression is shown in Equation (14).

$$\begin{cases} V'_{o1} = U_o M_2 \left(1 - 2\theta\right) \sin\left(wt\right) + n'_1\left(t\right) \\ V'_{o2} = U_o M_2 \left(1 + 2\theta\right) \sin\left(wt\right) + n'_2\left(t\right) \end{cases} \qquad (14)$$

In Equation (14), V'_{o1} and V'_{o2} denote the voltage outputs from the first and second filters, respectively, and $n'_1\left(t\right)$ and $n'_2\left(t\right)$ are the filtered noises from the first and second filters, respectively. The two signals from the filter outputs are phase adjusted by using a 90°phase shifter, and these signals are then fed to the computer via a data acquisition card. On the computer, specific signal processing software performs a double correlation detection operation, as previously described, to measure the amplitude of the signal [23]. This allows the angular offset corresponding to the measured current to be calculated, and subsequently the actual current value, with the expression shown in Equation (15).

$$i = \frac{\theta}{NV} = \frac{1}{2NV} \cdot \frac{V'_{o2} - V'_{o1}}{\left(V'_{o2} + V'_{o1}\right)} \qquad (15)$$

In Equation (15), i denotes the DC to be measured and its harmonics [24].

4. SIMULATION ANALYSIS OF THE IMPROVED OPTICAL DC TRANSFORMER MODEL

In order to analyse the simulation effect of the improved optical DC transformer model, the simulation effect of the improved sensing unit material based on TGG crystals is analysed.

4.1. Simulation Analysis of Improved Sensing Unit Material Based on TGG Crystals

The performance of TGG crystals for sensing applications is evaluated using a Faraday optics experimental setup, which fo-
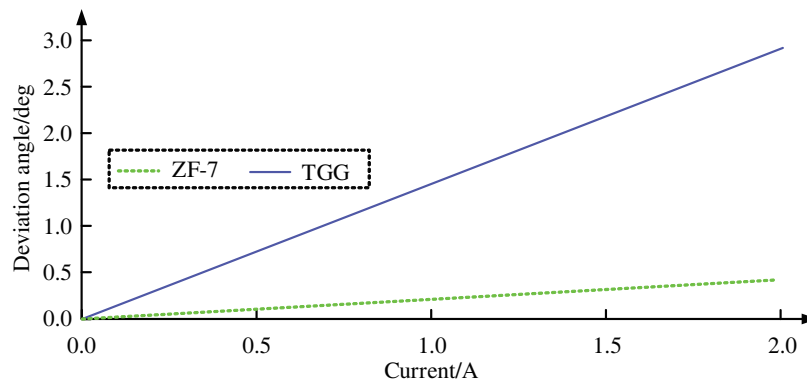
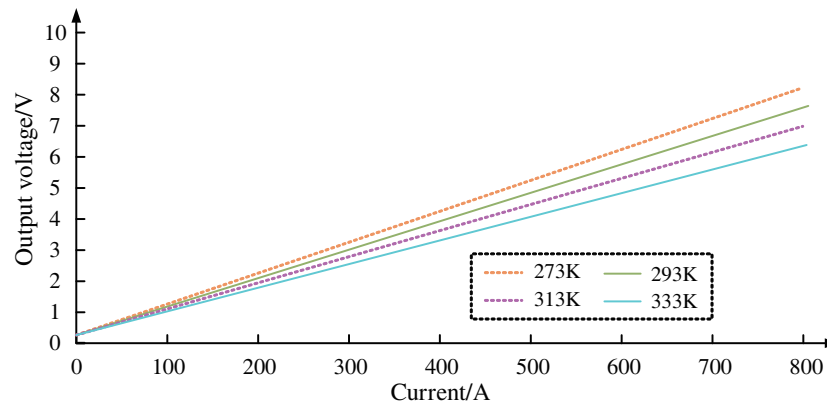**FIGURE 4**. Faraday optical experiment results.

FIGURE 5. Output characteristic curves at different temperatures.

cuses on measuring the deflection angle produced by the Faraday effect by means of a polarised light analyser. In general, the commonly used sensing material for optical current transformers is ZF-7, a cost-effective, antimagnetic magneto-optical glass with a small Fielder's constant but good temperature stability. TGG crystals are selected in standard sizes to ensure surface quality and transparency. ZF-7 magneto-optical glass is used as a comparison material, and samples of similar size and excellent quality are selected. Controllable electromagnets are sued to provide a uniform magnetic field. A laser light source with moderate wavelength is used to ensure beam stability and monochromaticity. The light emitted by the laser source is converted into polarized light through a polarizer and then passes through the TGG crystal or ZF-7 sample placed in the appropriate position. The light passing through the sample is then passed through the analyzer and finally received by the photodetector. Apply a uniform magnetic field in the sample area, with the direction of the magnetic field parallel to the direction of light propagation. The magnetic field intensity is adjustable to evaluate the Faraday rotation effect of materials under different magnetic field intensities. Accurately measure the rotation angle of polarized light passing through the sample after passing through the analyzer using a rotary table. Test the system without applying a magnetic field to ensure the accuracy of the measurement system when there is no rotation angle. Gradually increase the magnetic field intensity and record the Faraday ro-

tation angles generated by TGG and ZF-7 samples under different magnetic field intensities. Accurately record the magnetic field intensity corresponding to the rotation angle to prepare data for subsequent analysis. To ensure the accuracy and stability of the data, multiple measurements were taken on TGG and ZF-7 samples under the same conditions, and the results were recorded. In the experiment, the advantages of TGG were verified by comparing the performances of TGG crystals with those of ZF-7 glass, and the Faraday deflection angles produced by them were first measured, and the results of the experiment are shown in Fig. 4.

As can be seen from the data in Fig. 4, the sensing unit exhibits high linearity in the measurements, whether using TGG crystals or ZF-7 magneto-optical glass. However, the sensor using the TGG crystal significantly improves this Faraday deflecting angle contrast to the ZF-7 glass, which helps to increase SNR. In addition, based on the fitted characteristic curve's slope, the TGG crystal enhances the measurement sensitivity of the sensor obviously. Next, the output response of the TGG crystal was measured at different temperatures when the current was varied from 100 A to 800 A. The results are displayed in Fig. 5.

According to Fig. 5, the slope of the output characteristic curve of the TGG crystal decreases as the temperature rises, which indicates that its Fielder's constant also decreases. In order to explore the effect of temperature change on the spe-
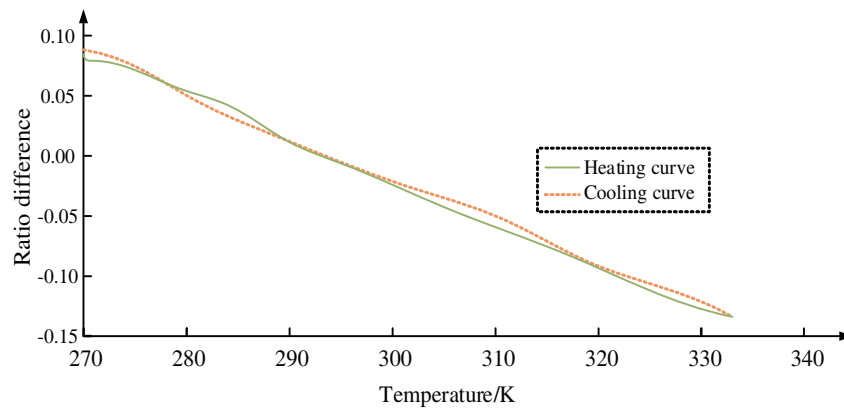
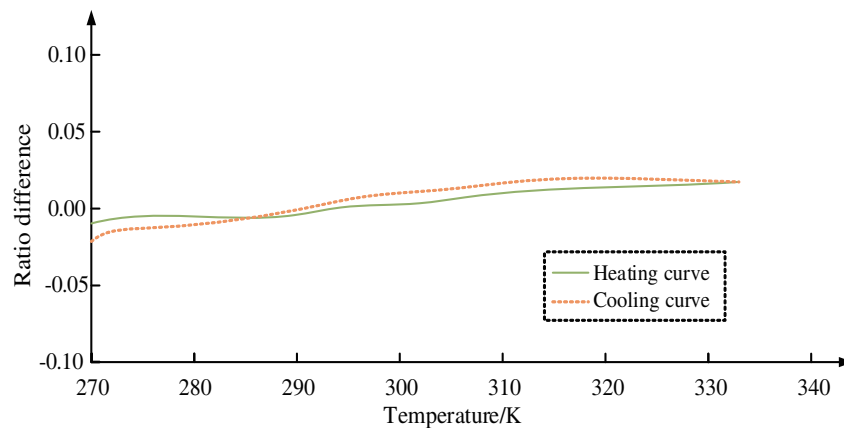**FIGURE 6**. Difference before temperature compensation.

FIGURE 7. Temperature compensation ratio difference.

cific difference and the feasibility of the temperature compensation strategy, the study set 600 A as the test current, used the measurement data at 293 K as the reference point, and the temperature varied between 273 K and 333 K. It was assumed that the specific difference was triggered by the temperature exclusively by both warming up and cooling down pathways. The evolution of the specific difference with temperature is shown in Fig. 6.

The variation of the specific difference during warming and cooling demonstrated in Fig. 6 shows a high degree of consistency, and its trend coincides with that of the variation of the Fielder's constant of TGG crystals with temperature. This confirms that the temperature instability of the measurement system is mainly caused by the temperature sensitivity of the TGG crystal. Temperature fluctuations cause significant disturbances to accurate measurements, and thus temperature compensation needs to be implemented to counteract this effect. The results of the adjusted measurement ratio difference after applying the proposed temperature compensation strategy are shown in Fig. 7.

In Fig. 7, the results show that the adopted temperature compensation method effectively attenuates the effect of temperature variation on the measurement accuracy in both warming and cooling cases.

4.2. Simulation Analysis Based on Add-Window Bicorrelation Detection Algorithm

PSCAD simulation software is used to create models of high-voltage direct current transmission systems and perform transient algorithm simulations. Build a high-voltage direct current transmission system model in PSCAD, including necessary components such as transmission lines, loads, and control systems. Window functions include integral period window functions and non integral period window functions, used for transient signal processing. Set PSCAD simulation parameters, such as simulation time (at least two seconds), as well as the type and frequency of data to be recorded. The results are shown in Fig. 8.

It can be seen from Fig. 8 that the implemented bicorrelation detection algorithm does not perform well in noise reduction if the rectangular window is set too short. Increasing the length of the window significantly improves the noise reduction. However, when the window is too large, the detection error for the mutation point rises, which indicates that too long a window length degrades the measurement performance of transient signals. In the field of signal processing, the selection of window length L is a trade-off between noise reduction performance and time resolution. The window length is crucial for achieving the performance of dual correlation detection algorithms in noise cancellation and mutation point detection. A longer win-
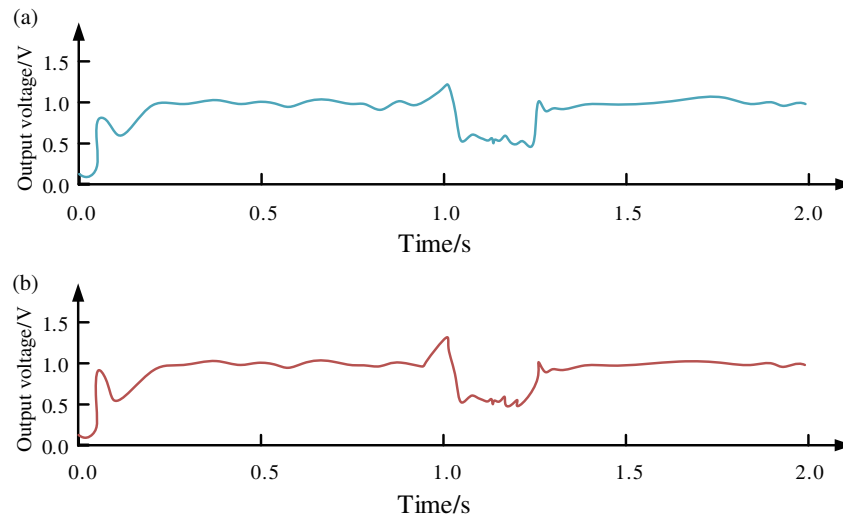
FIGURE 8. Simulation results of whole period and non-whole period window functions. (a) Full cycle window simulation results (window length $L = 500$). (b) Simulation results of non integer period window (window length $L = 125$).
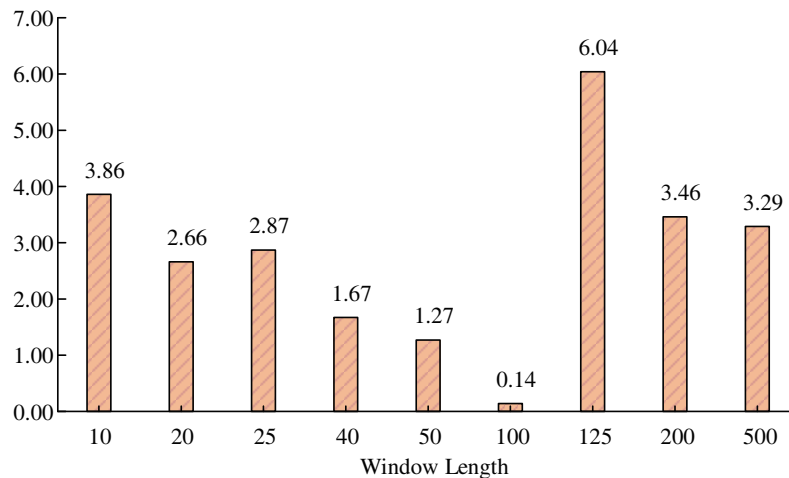

FIGURE 9. Measurement error results for different time windows.

dow length helps improve the noise reduction effect, as it increases the smoothness of the signal and reduces the impact of random noise by averaging more data points. A longer window length also helps to improve the detection accuracy of transient events, such as sudden changes in current. A shorter window allows the algorithm to respond faster to changes in the signal, thereby improving temporal resolution. If the window length is reduced to its limit, although the time resolution is improved, the impact of noise will increase, which will lead to a decrease in signal quality, especially in noisy environments. Choosing a window of moderate length is to find a balance between reducing noise and improving detection accuracy. The adjustment of window length significantly affects the overall performance of the algorithm, including its noise reduction ability and accuracy in detecting mutation points. Ideally, the window length should be finely adjusted according to the specific application requirements and signal properties to achieve the best performance balance. Therefore, the window length has not been reduced to the limit, but the optimal choice has been made based

on algorithm performance and application requirements. In relay protection and other applications using transient signals, the focus is usually on the accurate measurement of current mutations during fault occurrence. Therefore, the measurement errors at the point of mutation corresponding to different window lengths are shown in Fig. 9.

It can be seen through Fig. 9 that when the window lengths are similar, the measurement error caused by the non-integer period window exceeds the error caused by the integer period window, which indicates that higher accuracy can be obtained by using the integer period window for the measurement. Therefore, a window length of 100 samples was chosen for the study, and by comparing the mutation points of the current signals before and after denoising, it was found that due to the delay of the algorithm itself, the mutation points of the denoised signals had a time error about 1 ms compared to the ideal signal. As far as the amplitude error is concerned, the measurement error of the current spike point is about 0.2. The simulation re-
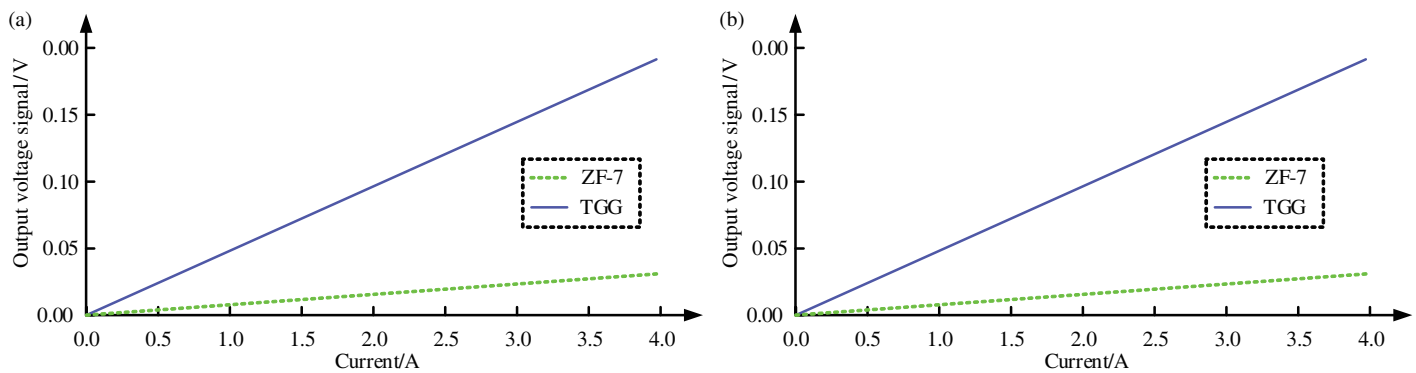
FIGURE 10. Fitting curves of measurement data generated from two materials. (a) Fit curve. (b) Measurement value.
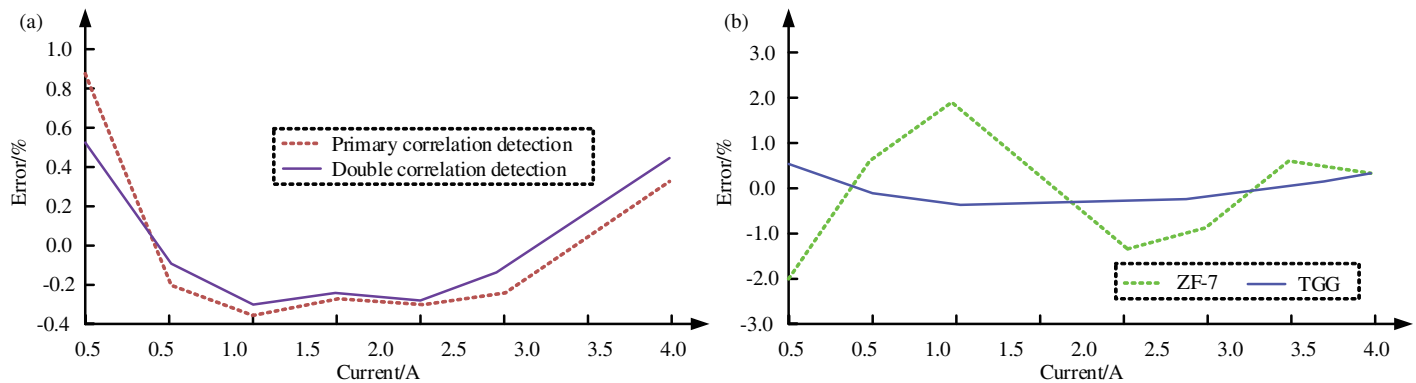

FIGURE 11. Error results of algorithms and crystals. (a) Algorithm. (b) Measurement error of crystal materials.

sults show that this delay and amplitude error is acceptable and meets the requirement of transient measurement.

4.3. Optical DC Transformer Model Performance Analysis

On the experimental platform of the constructed DC measurement system, the steady state experiments test the current derived from the relay protection test equipment, ranging from 0 to 4 A. Firstly, a comparative analysis of the materials is carried out to compare the performance of the ZF-7 magneto-optical glass commonly used in engineering with the TGG magneto-optical crystal recommended by the research as the sensor material, under the premise of using the same signal processing method — dual correlation detection algorithm. The performance of the sensor material is compared with that of the TGG magneto-optical crystal recommended in the study. The fitted curves of the measurement data generated by the two materials as the test current was varied from 0 to 4 A are shown in Fig. 10.

As can be seen from the analysis of Fig. 10, the characteristic curves obtained from the practically constructed measurement system are consistent with the results obtained from the previously studied Faraday effect experiment, verifying the similarity of the slopes of the two materials. The Faraday effect describes the influence of a material on the polarization state of light in a magnetic field, where the angular rotation of the material is proportional to the light passing through the material, the specific magneto-optical constant of the material, and the applied magnetic field strength. When using materials such as

TGG crystals as sensing elements in measurement systems, the performance analysis of the system usually focuses on two key parameters: slope and amplitude of voltage output. The slope is directly related to the Verdet constant of a material, which is a physical quantity that describes the material's magneto-optical response ability. The larger the Verdet constant is, the greater the polarization rotation angle is generated by the material for the same strength magnetic field, resulting in a higher slope. The slope also depends on the strength of the applied magnetic field. Within a certain range, a stronger magnetic field will generate greater polarization rotation, thereby increasing the slope. Upon comparison, it is found that the system applying TGG crystals exhibits better linear characteristics, with a significant improvement in the curve slope and output voltage amplitude, which will help to enhance the output SNR and sensitivity of the measuring system.

Next, error experiments were conducted to compare the effectiveness of the one- and two-fold correlation detection algorithms in reducing measurement errors when using TGG crystals as the sensing material. Continuing with the in-depth comparison, the results of comparing the error when using TGG crystals with ZF-7 magneto-optical glass as the sensing material under the twofold correlation detection algorithm are shown in Fig. 11.

The design purpose of primary and secondary correlation detection algorithms is to improve measurement accuracy and reduce errors. TGG crystals may perform better than ZF-7 magneto-optical glass in terms of error reduction due to its
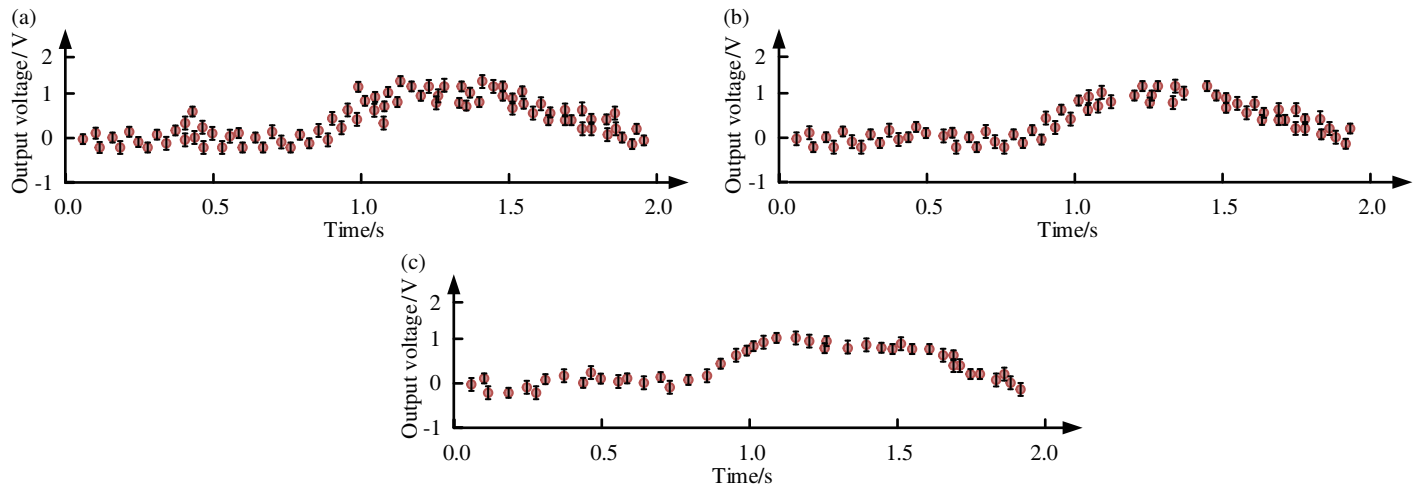
(a)

(b)

(c)

FIGURE 12. Three types of output signal processing results. (a) Output signals without signal processing. (b) Output signal of standard current transformer. (c) Output signal of optical DC measurement device.

higher Verdet constant and better utilization of magneto-optical effects. This will result in lower error values on the error curve and a trend closer to actual measurement data on the fitting curve. In Fig. 11, the twofold correlation detection algorithm can reduce the measuring error more effectively than the one fold correlation detection algorithm under the same sensing material condition. Compared with ZF-7 magneto-optical glass, TGG crystal as sensing material can further decrease the measuring error. Taken together, the DC measuring system using the TGG crystal and twofold correlation detecting algorithm can control the error to about 0.3 s.

In the transient experiments, an inrush current generator was used to generate an inrush current with a rise time of 30 microseconds, which was used as the transient current under test. For benchmark comparison, Rogowski coils were used as standard current transformers in the experiments. The comparison of the output of the optical DC measurement device without signal processing, the optical measurement device after signal processing, and the Rogowski coil is presented in Fig. 12.

The analysis of the results shows that the optical DC measurement device, after the designed signal processing, excels in its noise reduction capability. The waveform obtained from optical measurement system is very close to the shape of the waveform obtained from the Rogowski coil, showing the effectiveness of the signal processing. In addition, the error of the amplitude of the waveform measured by the system was controlled within 0.5%, confirming that the measurement system successfully restored the waveform and amplitude of the transient current and met the accuracy requirements of the experiment.

5. CONCLUSION

With the continuous development of DC transmission technology, especially high-voltage DC transmission technology, the accuracy and stability of the current transformer is required to be higher. The study, in order to cope with the challenge of low SNR of the output signal, uses TGG crystals with high

Fielder's constant. Based on the weak signal detection technique, a dichroic correlation detection method with added windows is proposed. Simulation results show that the slope of the output characteristic curve of the TGG crystal decreases with increasing temperature, and the system applying the TGG crystal helps to enhance the output SNR and sensitivity of the measuring system. The twofold correlation detecting algorithm is more effective in reducing the measurement error under the same sensing material conditions compared with the one fold correlation detecting algorithm. This system's measured waveform amplitude error is controlled within 0.5%, which confirms that the measurement system successfully restores the waveform and amplitude of the transient current and meets the accuracy requirements of the experiment. Overall, the study of optical DC transformers incorporating improved sensor materials and signal processing techniques is of great significance for enhancing the performance and reliability of power systems. There are still shortcomings in this research, such as the lack of incorporating a closed-loop control system, which requires further verification of the stability of the system.

REFERENCES

[1] Cui, S., J.-H. Lee, J. Hu, R. W. D. Doncker, and S.-K. Sul, "A modular multilevel converter with a zigzag transformer for bipolar MVDC distribution systems," *IEEE Transactions on Power Electronics*, Vol. 34, No. 2, 1038–1043, 2019.

[2] Luo, X., J. Tang, C. Pan, and Y. Zhang, "Contribution of free iron particles to PD characteristics in flowing transformer oil at DC voltages," *IET Generation, Transmission & Distribution*, Vol. 14, No. 2, 294–300, 2020.

[3] Durrani, A., A. Javaid, S. Lee, and J. Ha, "Optical rotary junction incorporating a hollow shaft DC motor for high-speed catheter-based optical coherence tomography," *Optics Letters*, Vol. 45, No. 2, 487–490, 2020.

[4] Shi, S., F. Zhuo, Y. Zhu, S. Cheng, and F. Wang, "Research on control strategy of MMC DC power electronic transformer based on DAB mode," *IET Generation, Transmission & Distribution*, Vol. 14, No. 21, 4694–4702, 2020.

[5] Zhuo, C., X. Zhang, X. Zhang, and X. Yang, "Research on fault current limitation and active control for power electronic transformer in direct current grid," *IET Generation, Transmission & Distribution*, Vol. 15, No. 1, 121–134, 2021.

[6] Wang, C., K. Jia, T. Bi, Z. Xuan, and R. Zhu, "Transient current curvature based protection for multi-terminal flexible DC distribution systems," *IET Generation, Transmission & Distribution*, Vol. 13, No. 15, 3484–3492, 2019.

[7] Zhang, W., M. Armstrong, and M. A. Elgendy, "Mitigation of DC current injection in transformer-less grid-connected inverters using a voltage filtering DC extraction approach," *IEEE Transactions on Energy Conversion*, Vol. 34, No. 1, 426–434, 2019.

[8] Canturk, S., M. E. Balci, M. H. Hocaoglu, and A. K. Koseoglu, "Performance analysis of three-phase five-leg transformers under DC bias using a new frequency-dependent reluctance-based model," *IET Generation, Transmission & Distribution*, Vol. 16, No. 12, 2455–2465, 2022.

[9] Lee, H.-S., B. Kang, W.-S. Kim, and S.-J. Yoon, "Reduction of input voltage/current ripples of boost half-bridge DC-DC converter for photovoltaic micro-inverter," *Solar Energy*, Vol. 188, 1084–1101, Aug. 2019.

[10] Achlerkar, P. D. and B. K. Panigrahi, "Assessment of DC offset in fault current signal for accurate phasor estimation considering current transformer response," *IET Science, Measurement & Technology*, Vol. 13, No. 3, 403–408, 2019.

[11] Geng, J., R. A. Badcock, and C. W. Bumby, "A wireless rectifier for inductively energizing high direct-current high-temperature superconducting magnets," *IEEE Transactions on Industrial Electronics*, Vol. 68, No. 4, 3273–3281, 2021.

[12] Belčević, N. M. and Z. N. Stojanović, "Algorithm for phasor estimation during current transformer saturation and/or DC component presence: Definition and application in arc detection on overhead lines," *IET Generation, Transmission & Distribution*, Vol. 14, No. 7, 1378–1388, 2020.

[13] Li, J. and J. Li, "Core form transformer topological duality based transient model validation for exciting current calculation within DC bias," *IET Generation, Transmission & Distribution*, Vol. 14, No. 15, 3099–3107, 2020.

[14] Silva, W. W. G., L. M. C. S. Hildever, M. C. G. Santos, F. Estrada, and J. Holanda, "Analyzing the magnetic influence on magneto-optical interactions," *Journal of Superconductivity and Novel Magnetism*, Vol. 36, No. 3, 951–955, 2023.

[15] Royintarat, T., P. Seesuriyachan, D. Boonyawan, E. H. Choi, and W. Wattanutchariya, "Mechanism and optimization of non-thermal plasma-activated water for bacterial inactivation by underwater plasma jet and delivery of reactive species underwater by cylindrical DBD plasma," *Current Applied Physics*, Vol. 19, No. 9, 1006–1014, 2019.

[16] Miller, D. C., K. E. Hurst, A. Sinha, J. Qian, S. L. Moffitt, S. Uličná, L. T. Schelhas, and P. Hacke, "Quantifying optical loss of high-voltage degradation modes in photovoltaic modules using spectral analysis," *Progress in Photovoltaics*, Vol. 31, No. 8, 840–861, 2023.

[17] Vidyasagar, R., O. A. Santos, J. Holanda, R. O. Cunha, F. L. A. Machado, P. R. T. Ribeiro, A. R. Rodrigues, J. B. S. Mendes, A. Azevedo, and S. M. Rezende, "Giant zeeman shifts in the optical transitions of yttrium iron garnet thin films," *Applied Physics Letters*, Vol. 109, No. 12, 122402, 2016.

[18] Tavsanoglu, T., E. O. Zayim, O. Agirseven, S. Yildirim, and O. Yucel, "Optical, electrical and microstructural properties of SiC thin films deposited by reactive DC magnetron sputtering," *Thin Solid Films*, Vol. 674, 1–6, Mar. 2019.

[19] Hildever, L., T. Ferro, A. Dias, A. José, F. Estrada, and J. Holanda, "Detecting magneto-optical interactions in nanostructures," *ArXiv Preprint ArXiv:2401.03294*, 2024.

[20] Emami, H. and A. A. Sharifi, "A novel bio-inspired optimization algorithm for solving peak-to-average power ratio problem in DC-biased optical systems," *Optical Fiber Technology*, Vol. 60, 102383, Dec. 2020.

[21] Lin, C.-W., J.-M. Chen, Y.-J. Lin, L.-W. Chao, S.-Y. Wei, C.-H. Wu, C.-C. Jeng, L.-M. Wang, and K.-L. Chen, "Magneto-optical characteristics of streptavidin-coated Fe_3O_4@Au core-shell nanoparticles for potential applications on biomedical assays," *Scientific Reports*, Vol. 9, No. 1, 16466, 2019.

[22] Chen, Y., W. Fu, H. Lin, and S. Niu, "A passive negative magnetic reluctance structure-based kHz transformer for improved DC magnetic bias withstanding," *IEEE Transactions on Power Electronics*, Vol. 38, No. 1, 717–727, 2023.

[23] Sarsen, A. and C. Valagiannopoulos, "Robust polarization twist by pairs of multilayers with tilted optical axes," *Physical Review B*, Vol. 99, No. 11, 115304, 2019.

[24] Wellendorf, A., P. Tichelmann, and J. Uhl, "Performance analysis of a dynamic test bench based on a linear direct drive," *Archives of Advanced Engineering Science*, Vol. 1, No. 1, 55–62, 2023.